Detector Array Readout with Traveling Wave Amplifiers

(Article begins on next page)

Detector Array Readout with Traveling Wave Amplifiers

A. Giachero[1,2] · C. Barone[3,4] · M. Borghesi[1,2] · G. Carapella[3,4] · A. P. Caricato[5,6] ·
I. Carusotto[7,8,9] · W. Chang[19] · A. Cian[9,10] · D. Di Gioacchino[11] · E. Enrico[9,12] ·
P. Falferi[9,10,13] · L. Fasolo[12,14] · M. Faverzani[1,2] · E. Ferri[1,2] · G. Filatrella[4,15] ·
C. Gatti[11] · D. Giubertoni[9,10] · A. Greco[12,14] · C. Kutlu[19,20] · A. Leo[5,6] · C. Ligi[11] ·
G. Maccarrone[11] · B. Margesin[9,10] · G. Maruccio[5,6] · A. Matlashov[19] · C. Mauro[4] ·
R. Mezzena[9,16] · A. G. Monteduro[5,6] · A. Nucciotti[1,2] · L. Oberto[9,12] · S. Pagano[3,4] ·
V. Pierro[4,17] · L. Piersanti[11] · M. Rajteri[12,18] · S. Rizzato[5,6] · Y. K. Semertzidis[19,20] ·
S. Uchaikin[19] · A. Vinante[9,10,13]

Abstract

Reducing noise to the quantum limit over a large bandwidth is a fundamental requirement for future applications operating at millikelvin temperatures, such as the neutrino mass measurement, the next-generation X-ray observatory, the CMB measurement, the dark matter and axion detection, and the rapid high-fidelity readout of superconducting qubits. The read out sensitivity of arrays of microcalorimeter detectors, resonant axion-detectors, and qubits, is currently limited by the noise temperature and bandwidth of the cryogenic amplifiers. The Detector Array Readout with Traveling Wave Amplifiers project has the goal of developing high-performing innovative traveling wave parametric amplifiers with a high gain, a high saturation power, and a quantum-limited or nearly quantum-limited noise. The practical development follows two different promising approaches, one based on the Josephson junctions and the other one based on the kinetic inductance of a high-resistivity superconductor. In this contribution, we present the aims of the project, the adopted design solutions and preliminary results from simulations and measurements.

Keywords Quantum noise · Parametric amplifier · Traveling wave · Detector array read out · Qubits read out

✉ A. Giachero
andrea.giachero@mib.infn.it

Extended author information available on the last page of the article

⚛ Springer

1 Introduction

A wide range of quantum technologies rely on the faithful detection of microwave signals at millikelvin temperatures. This includes quantum computing with superconducting [1] and spin [2] qubits, multiplexed readout of particle and astronomical detectors (TESs [3, 4] and MKIDs [5, 6]) or the search for axionic dark matter with microwaves cavities [7, 8]. These experiments often use amplifiers based on semiconductors (HEMT) with an high gain but with a noise 10–40 times above the standard quantum limit, the fundamental limit imposed by quantum mechanics [9]. At microwave frequencies, Josephson Parametric Amplifiers (JPA) [10] have demonstrated quantum-limited noise and are currently used in axion search and qubit read out. Nevertheless, JPAs can provide only a limited bandwidth (few hundred megahertz) and still cannot read out more than a handful of devices simultaneously. This represents a limitation for addressing the needs of the above-mentioned applications. An alternative and innovative solution is based on parametric amplification exploiting the traveling wave concept. A Traveling Wave Parametric Amplifiers (TWPA) is designed by exploiting the signal (nonlinear) response of reactive parts (typically inductance) in a superconducting circuit. A large pump tone modulates this inductance, coupling the pump (f_p) to a signal (f_s) and idler (f_i) tone via frequency mixing such that $2f_p = f_s + f_i$ (4-wave mixing, 4 WM) or $f_p = f_s + f_i$ (3-wave mixing, 3 WM). The nonlinear inductance can be implemented by means of Josephson Junction (JJ) and Kinetic Inductance (KI) of superconductors. The relationship is, at the first order, $L(I) = L_0[1 + (I/I_c)^2]$, where I_c is the superconductor critical current. At $I < I_c$, junctions are dissipationless and act as nonlinear inductors.

In recent times, the concept of a parametric amplifier with microwaves travelling along a transmission line with embedded Josephson junctions (TWJPA) was developed in several groups [11, 12]. These devices operate at near quantum-limited noise performance and are used to readout superconducting qubit [13]. TWPA based on KI, called Dispersion-engineered Traveling Wave Kinetic Inductance (DTWKI) parametric amplifier or Kinetic Inductance Traveling Wave Parametric amplifier (KI-TWPA or in short-form KIT), was originally proposed by J. Zmuidzinas group at Caltech in 2012 and the first demonstrators have been produced after few years of development by Caltech [14] and NIST [15]. Recent results showed a noise very close to the quantum limited performance with a gain around 15 dB over a 5 GHz bandwidth [16–18]. These results highlight the potential of parametric amplifiers. However, they also show that significant progress is still needed to achieve the required gain, bandwidth, and noise performance with acceptable power dissipation.

The Detector Array Readout with Traveling Wave Amplifiers (DARTWARS) is a three-year project funded by the Italian Institute for Nuclear Physics (INFN) starting from 2021 that aims to fulfil these requirements. The technical goal is to achieve a gain value around 20 dB, comparable to HEMT, a high saturation power (around -50 dBm), and a quantum limited or nearly quantum limited noise ($T_N < 600$ mK) in the 4–8 GHz (C-band) and 8–12 GHz frequency bands .

These features will lead to reading out large arrays of detectors or qubits with no noise degradation. The development of two different approaches is surely more demanding in terms of time and costs but, for sure, is the best way to maximize the success of the action.

2 TWJPA Design

Josephson junctions based Traveling Wave Parametric Amplifiers are composed by a coplanar waveguide (CPW) embedding a chain elementary cells containing Josephson Junctions (eg. rf-SQUIDs). The nonlinear behaviour can be tuned using an external magnetic field or a DC bias that flows in the signal line, allowing it to work as a three-wave mixer [19] or a four-wave mixer. The DARTWARS design follows the quantum model developed by INRiM [20, 21], a coupled mode equation approach to describe the behaviour of a TWJPA in the few-photons or even single-photon level.

To avoid power leakage into higher frequency tones the CPWs are equipped with a modified dispersion relation following two different approaches, the Resonant Phase Matching (RPM) and the Quasi-Phase Matching (QPM) techniques. RPM uses a reduced plasma frequency mixed to a periodic load of LC resonators to create mismatch among the traveling tones, in order to suppress higher harmonic generation, and re-phase just the signal tone that is meant to be amplified through the opening of a bandgap in the dispersion relation [22]. On the contrary, QPM uses a mix of low plasma frequency and a sign modulation of the nonlinearity into the medium to suppress higher harmonic generation and stimulate amplification by changing the phase of the traveling waves of π after a coherence length has been reached [23].

During 2021 INRiM developed a modified version of the quantum model [20], which implements in its mathematical structure the modified dispersion relation given by the RPM technique. The study highlights how the presence of the RPM helps reduce the phase mismatch between the traveling tones given by the low plasma frequency (35 GHz), enhancing the overall gain of several dB respect to the case where RPM is not used. Moreover, a numerical study on the RPM and QPM approach has been performed through a Coupled Mode Equations (CME) method [24]. The CME method takes into account modes at frequency as high as the fifth pump harmonic, meaning that the power dispersion of the pump into higher harmonics can be quantitatively studied and monitored. Figure 1 reports the results of these numerical simulations for the RPM (left) and QPM (right) schemes optimized to work at a pump frequency around 12.7 GHz. In both schemes the 50 Ω matched devices consist of a repetition of 900 (RPM) or 1300 (QPM) rf-SQUID based cells composed by a Josephson junction (critical current $I_c = 2\,\mu A$) in parallel with a geometrical inductance ($L_g = 100$ pH). The effects of the introduction of LC resonator in the RPM scheme and the modulation of the nonlinearity sign via the exchange of the Josephson junction and the geometrical inductance in the QPM scheme are clearly visible in the dashed line reported in figure 1. The poling scheme maximize its effect by binary encoding a sinusoidal value of the nonlineariry with a period of 579 cells [23].
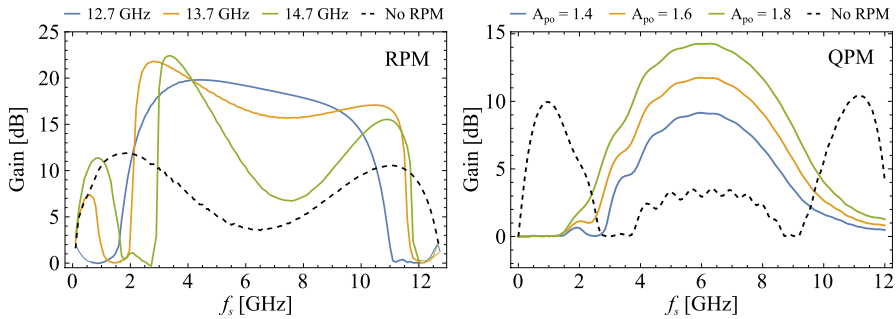
Fig. 1 (left) Gain in the 3WM regime as a function of signal frequency f_s for a JTWPA implementing the RPM scheme calculated for different pump frequencies by exploiting the Coupled Modes Equations approach (CME-2). (right) Gain in the Three-Wave Mixing regime as a function of signal frequency f_s for a JTWPA implementing the QPM scheme, calculated for different normalized pump amplitudes (A_{po}) by exploiting the Coupled Modes Equations approach (CME-2) (Color figure online)

The physical implementation of the circuit components occurred through electromagnetic simulations performed with the software Sonnet Suite. The RPM technique needs shunt resonators with resonant frequency very close to the pump frequency, hence in the range 10–15 GHz depending on the working band, and a reduced plasma frequency, around 35 GHz. These facts require the presence of large capacitances in the resonators and shunting the Josephson junctions, that can be reached by adding an extra layer of dielectric material in the layout so as to allow the use of parallel plate capacitors. The same result can be achieved using extended 2D planar resonators and large area Josephson junctions. The former approach allows reducing the areas of the Josephson junctions at the cost of adding a layer of dielectric material. The Sonnet Suite has been used to realise the physical layout of the devices in the presence and absence of the extra dielectric layer, that has been chosen to be SiO2 (loss tangent 10^{-3}) and a-Si:H (loss tangent 2.5×10^{-5} [25]), and to evaluate material dependent losses affecting the final added noise performances where two-level-systems play the significant role. The physical implementation of QPM-JTWPA does not require resonators but just a poling of the rf-SQUIDs and a reduced plasma frequency, that again can be reached by enlarging the area of the Josephson junctions and proper tuning of the oxidation process realizing the tunnel barrier.

3 TWJPA Fabrication

The preliminary characterization of the first TWJPA prototypes fabricated at INRiM highlighted the presence of unwanted effects ascribable to an inhomogeneity in the area of the fabricated Josephson Junctions (JJs). These first prototypes were fabricated exploiting a well-established nanofabrication technology based on electron beam lithography (EBL) on a double layer polymeric mask (bottom layer realized with the copolymer MMA(8.5)MAA EL11 and top layer realized with 950K PMMA A4, both by KayakuAM) followed by an Aluminium e-gun evaporation exploiting

the Niemeyer-Dolan technique. The realization of thousands of micrometric structures, such as those present in a TWJPA architecture, in the range of time in which the lithographic system is stable and predictable requires the use of a large beam current, causing a reduction in the pattern resolution and hence the origin of a spread in the areas of the JJs. To overcome this issue, in the first half of 2021, INRiM started to fabricate new TWJPAs exploiting a two-step lithography approach. The lithography of the components with a resolution bigger than 1 m were realized with an UV laser writer (PG-101 from Heidelberg) exploiting a polymeric mask realized with the reverse image photoresist AZ 5214 E from Microchemicals GmbH. To reach the desired resolution for this process over large areas, up to 2" diameter, many process parameters have been tuned (spinning protocol, power of the UV laser, bake time and temperature of the mask and time of the development). The second lithography step, reserved to the features smaller than 1 m, will be realized with EBL. This will guarantee the use of a small beam current and hence an increase in the resolution of the process. Moreover, to further reduce the JJ areas inhomogeneity due to the overlap of unpredictable rounded edges, a new design for these structures is under development. This design will exploit a new double layer mask made with LOR 20B and 950K PMMA A4, both from KayakuAM. Preliminary characterization of the lithography and development of this mask have been already performed during the first half of 2021. To realize TWJPA architectures that need the presence of a dielectric layer, during the first half of 2021 INRiM grown and characterized thin films of SiO2 and a-Si:H realized with an Inductively Coupled Plasma Chemical Vapour Deposition system (PlasmaPro 100 ICPCVD by Oxford Instruments). Several samples, realized at different substrate temperatures (from 200 to 350 °C), were preliminary analyzed with spectroscopic ellipsometric and FTIR (Fourier-transform infrared spectroscopy) measurement.

4 KI-TWPA Design

Traveling wave amplifiers require both momentum conservation, i.e., phase matching, and energy conservation for the pump, signal, and any idlers that are generated. For the KI-TWPA device, momentum conservation can be attained by i) dispersion engineering of the CPW with periodic loadings that create a frequency gap or by ii) an artificial transmission line, also known as a lumped-element transmission line, that uses lumped-element inductors and capacitors instead of the distributed inductances and capacitances in a conventional transmission line. The characteristic impedance of the transmission line is modified every one-sixth of a wavelength at a frequency slightly above the pump frequency f_p to form a wide stopband at $3f_p$. In addition, every third loading is modified in length (longer or shorter relative to the first two) to create a narrow stopband near f_p. Placed just below this narrow stopband, the pump tone picks up additional phase shift to fulfill the phase-matching condition, while its third harmonic is suppressed by the $3f_p$ stopband. As a result, exponential gain can be achieved over a broad bandwidth of more than one-half the pump frequency. CPW amplifiers, made in NbTiN, achieved 15 dB gain with a transmission line 2 m long [14]. More recent versions based on lumped

elements, and made of NbTiN, achieved comparable gains with a transmission line 33 cm long [17]. The advantage of the lumped element approach is that a shorter transmission line results in a higher fabrication yield [26]. In addition, longer CPW line means higher chances to have fabrication defects that could cause impedance mismatches in the line. These mismatches cause standing waves that, in turn, could cause large ripples in the gain profile. As a result, the amplifier chip heats up, due to the strong pump tone, creating an excess of thermal noise. Considering all of these advantages, the goal of the DARTWARS project is to design KI-TWPA prototypes as a weakly dispersive artificial transmission line implemented by lumped-element inductors and capacitors (see Fig. 2 as example).

5 KI-TWPA Fabrication

The first aim is to tune the fabrication process in order to realize parametric amplifiers in NbTiN with a critical temperature around $T_c = 15$ K [26] and a kinetic inductance around $L_k = 10$ pH/square [17]. To achieve these requirements a new sputtering system based on a KS 800 C Cluster provided by Kenosistec S.r.l. is currently being commissioned and tuned at the Fondazione Bruno Kessler-Center for Materials and Microsystems (FBK-CMM). The cluster is composed of two deposition chambers and a chamber for loading and transfers. Each deposition chamber is equipped with 4 Magnetron cathodes and turbomolecular pump able to reach a base vacuum of 5×10^{-9} mbar. The system is capable of handling 6" wafers and allows heating of substrates up to 400 °C. Deposition can be performed by reactive sputtering, by injecting Nitrogen, and by co-sputtering using two cathodes at the same time. In preliminary phases the system has been tested with deposition of Niobium (Nb) and Niobium nitride (NbN), finding a good match with the literature [27].

Most of the NbTiN film depositions have been done with the reactive sputtering technique using a target of $Nb_{0.66}Ti_{0.34}$ alloy which reduces the number of parameters to optimize. All films have been deposited on oxidized Si-wafers heated up to 400 °C. In these tests the chamber pressure was kept at 3×10^{-3} mbar with an Ar flow of 50 sccm while the N_2 flow was verified from 5 to 22.5 sccm. As shown in Fig. 3 the highest critical temperature of $T_c = 14.08$ K has been obtained at a low

Fig. 2 Circuital model of a unit cell of a superconducting artificial line made of CPW sections (not to scale). In the equivalent electrical circuit, each cell is composed by a series inductance L_d and two resonators with inductance L_f and capacitance to ground $C/2$ (Color figure online)
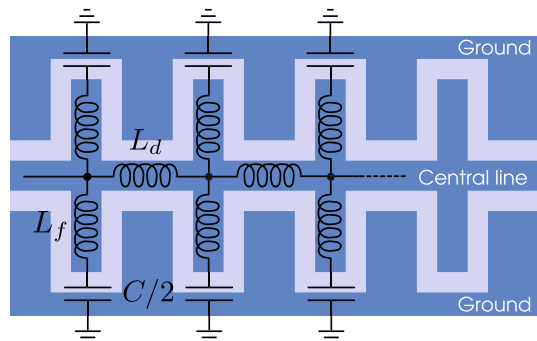
Fig. 3 (Top) Critical temperature as function of the nitrogen flow measured at cryogenic temperature for the deposited NbTiN films. (Bottom) Kinetic Inductance calculated based on the gap of the BCS theory and the sheet resistance and extrapolated for a film thickness of 30 nm (Color figure online)
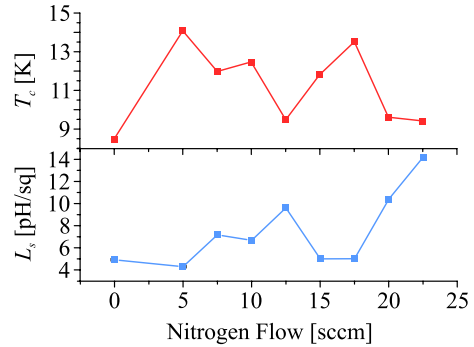
N_2 flow with a very narrow transition of 4 mK. This film resulted tensile with an estimated sheet resistance of 1312 $n\Omega$ m. The residual resistance ratio of the films resulted in the order of 1. For all films the kinetic inductance has been calculated based on the gap of the BCS theory and the sheet resistance and extrapolated for a film thickness of 30 nm , see Fig. 3. The next tests will explore in more detail the region with the highest transition temperature and to see if it is possible to obtain more compressive films by rising the process pressure. The first KI-TWPA prototypes are foreseen in 2022 and will be produced exploiting the optimized deposition and etching procedures developed during 2021.

6 Conclusion and Future Plans

TWPA are promising candidates as quantum limited microwave amplifiers for applications in fundamental physics experiments and quantum computing. The DART WARS project aims to develop high performances TWPA by exploring new design solutions, new materials, and advanced fabrication processes. The long-term goal is to demonstrate the readout with different sensors (Transition Edge Sensors, Microwave Kinetic Inductance Detectors, microwave cavities) and qubits, opening the concrete possibility to increase the sensitivity of the next generation of particle physics and quantum computing experiments.

References

1. P. Krantz et al., Appl. Phys. Rev. **6**, 021318 (2019). https://doi.org/10.1063/1.5089550
2. J. Stehlik et al., Phys. Rev. Appl. **4**, 014018 (2015). https://doi.org/10.1103/PhysRevApplied.4.014018
3. K.D. Irwin, G.C. Hilton, Top. Appl. Phys. **99**, 63–149 (2005). https://doi.org/10.1007/10933596_3
4. L. Gottardi, K. Nagayashi, Appl. Sci. **11**(9), 3793 (2021). https://doi.org/10.3390/app11093793
5. P. Day et al., Nature **425**, 817–821 (2003). https://doi.org/10.1038/nature02037
6. J. Zmuidzinas, Annu. Rev. Condens. Matter Phys. **3**(1), 169–214 (2012). https://doi.org/10.1146/annurev-conmatphys-020911-125022
7. D. Alesini et al., Phys. Rev. D **99**(10), 101101 (2019). https://doi.org/10.1103/PhysRevD.99.101101
8. N. Crescini et al., Phys. Rev. Lett. **124**(17), 171801 (2020). https://doi.org/10.1103/PhysRevLett.124.171801
9. C.M. Caves, Phys. Rev. D **26**, 1817 (1982). https://doi.org/10.1103/PhysRevD.26.1817
10. M.A. Castellanos-Beltran, K.W. Lehnert, Appl. Phys. Lett. **91**, 083509 (2007). https://doi.org/10.1063/1.2773988
11. K. O'Brien et al., Phys. Rev. Lett. **113**, 157001 (2014). https://doi.org/10.1103/PhysRevLett.113.157001
12. T.C. White et al., Appl. Phys. Lett. **106**, 242601 (2015). https://doi.org/10.1063/1.4922348
13. C. Macklin et al., Science **350**(6258), 307–310 (2015). https://doi.org/10.1126/science.aaa8525
14. H. Eom et al., Nat. Phys. **8**, 623–627 (2012). https://doi.org/10.1038/nphys2356
15. M.R. Vissers et al., Appl. Phys. Lett. **108**, 012601 (2016). https://doi.org/10.1063/1.4937922
16. N. Zobrist et al., Appl. Phys. Lett. **115**, 042601 (2019). https://doi.org/10.1063/1.5098469
17. M. Malnou et al., PRX Quantum **2**, 010302 (2021). https://doi.org/10.1103/PRXQuantum.2.010302
18. S. Shu et al., Phys. Rev. Res. **3**, 023184 (2021). https://doi.org/10.1103/PRXQuantum.2.010302
19. A.B. Zorin, Phys. Rev. Appl. **6**, 034006 (2016). https://doi.org/10.1103/PhysRevApplied.6.034006
20. A. Greco et al., arXiv:2009.01002 [cond-mat.supr-con]
21. AL. Fasolo et al., arXiv:2109.14924 [cond-mat.supr-con]
22. K. O'Brien et al., Phys. Rev. Lett. **113**, 157001 (2014). https://doi.org/10.1103/PhysRevLett.113.157001
23. A.B. Zorin, Appl. Phys. Lett. **118**, 222601 (2021). https://doi.org/10.1063/5.0050787
24. T. Dixon et al., Phys. Rev. Appl. **14**, 034058 (2020). https://doi.org/10.1103/PhysRevApplied.14.034058
25. A. Bruno et al., Phys. Procedia **36**, 245–249 (2012). https://doi.org/10.1016/j.phpro.2012.06.154
26. S. Chaudhuri et al., Appl. Phys. Lett. **110**, 152601 (2017). https://doi.org/10.1063/1.4980102
27. N. Pinto et al., Sci. Rep. **8**, 4710 (2018). https://doi.org/10.1038/s41598-018-22983-6

Springer

Authors and Affiliations

A. Giachero[1,2] · C. Barone[3,4] · M. Borghesi[1,2] · G. Carapella[3,4] · A. P. Caricato[5,6] ·
I. Carusotto[7,8,9] · W. Chang[19] · A. Cian[9,10] · D. Di Gioacchino[11] · E. Enrico[9,12] ·
P. Falferi[9,10,13] · L. Fasolo[12,14] · M. Faverzani[1,2] · E. Ferri[1,2] · G. Filatrella[4,15] ·
C. Gatti[11] · D. Giubertoni[9,10] · A. Greco[12,14] · C. Kutlu[19,20] · A. Leo[5,6] · C. Ligi[11] ·
G. Maccarrone[11] · B. Margesin[9,10] · G. Maruccio[5,6] · A. Matlashov[19] · C. Mauro[4] ·
R. Mezzena[9,16] · A. G. Monteduro[5,6] · A. Nucciotti[1,2] · L. Oberto[9,12] · S. Pagano[3,4] ·
V. Pierro[4,17] · L. Piersanti[11] · M. Rajteri[12,18] · S. Rizzato[5,6] · Y. K. Semertzidis[19,20] ·
S. Uchaikin[19] · A. Vinante[9,10,13]

[1]   Department of Physics, University of Milano Bicocca, 20126 Milan, Italy

[2]   INFN - Milano Bicocca, 20126 Milan, Italy

[3]   Department of Physics, University of Salerno, 84084 Fisciano, Salerno, Italy

[4]   INFN - Napoli, Salerno Group, 84084 Fisciano, Salerno, Italy

[5]   Department of Physics, University of Salento, 73100 Lecce, Italy

[6]   INFN-Sezione di Lecce, 73100 Lecce, Italy

[7]   INO-CNR BEC Center, 38123 Povo, Trento, Italy

[8]   Department of Physics, University of Trento, 38123 Povo, Trento, Italy

[9]   INFN - Trento Institute for Fundamental Physics and Applications, 38123 Povo, Trento, Italy

[10]   Fondazione Bruno Kessler, 38123 Povo, Trento, Italy

[11]   INFN - Laboratori Nazionali di Frascati, 00044 Frascati, Rome, Italy

[12]   INRiM - Istituto Nazionale di Ricerca Metrologica, 10135 Turin, Italy

[13]   IFN-CNR, 38123 Povo, Trento, Italy

[14]   Polytechnic University of Turin, 10129 Turin, Italy

[15]   Department of Science and Technology, University of Sannio, 82100 Benevento, Italy

[16]   Department of Physics, University of Trento, 38123 Povo, Trento, Italy

[17]   Department of Engineering, University of Sannio, 82100 Benevento, Italy

[18]   INFN - Torino, 10125 Turin, Italy

[19]   Center for Axion and Precision Physics Research, Institute for Basic Science (IBS),
       Daejeon 34051, Republic of Korea

[20]   Department of Physics, Korea Advanced Institute of Science and Technology (KAIST),
       Daejeon 34141, Republic of Korea